Solar-Terrestrial Physics. 2020. Vol. 6. Iss. 4. P. 44–49. DOI: 10.12737/stp-64202007. © 2020 G.A. Kotova, M.I. Verigin, T. Gombosi, K. Kabin. Published by INFRA-M Academic Publishing House
Original Russian version: G.A. Kotova, M.I. Verigin, T. Gombosi, K. Kabin, published in Solnechno-zemnaya fizika. 2020. Vol. 6. Iss. 4. P. 51–58. DOI: 10.12737/szf-64202007. © 2020 INFRA-M Academic Publishing House (Nauchno-Izdatelskii Tsentr INFRA-M)

ANALYTICAL MODEL OF THE PLANETARY BOW SHOCK FOR VARIOUS MAGNETIC FIELD DIRECTIONS BASED ON MHD CALCULATIONS

G.A. Kotova
Space Research Institute of RAS,
Moscow, Russia, kotova@iki.rssi.ru, gala5486@mail.ru

M.I. Verigin[†]
Space Research Institute of RAS,
Moscow, Russia

T. Gombosi
University of Michigan,
Ann Arbor, Michigan, United States, tamas@umich.edu

K. Kabin
Royal Military College of Canada,
Kingston, Ontario, Canada, Konstantin.Kabin@rmc.ca

Abstract. Study of physical processes in plasma near planets often requires knowledge of the position and shape of the planetary bow shock. Empirical models are usually used since theoretical MHD and kinetic models consume too much computer time and cannot be used to track fast processes. M.I. Verigin proposed a semi-empirical approach based on the use of exact theoretical expressions with a small number of parameters, which have a clear physical meaning. These parameters are estimated by fitting experimental data or detailed MHD calculations. A model of the bow shock near an arbitrary-shaped obstacle has previously been developed for a gas-dynamic flow. This model can be applied to any sonic Mach numbers and large values of the Alfven Mach number. In addition, the asymptotic Mach cone — the angle of inclination of the shock wave at an infinite distance from the planet — has been calculated analytically in the MHD approximation. In this paper, we propose a model of the bow shock for any direction of the magnetic field with respect to the upcoming flow and for any Mach numbers. Parameters of the model are the distance of the nose point from the obstacle, radius of curvature and bluntness of the bow shock at the nose point, a parameter related to the transition to the asymptotic downstream slope of the shock, and a skewing angle appearing when the interplanetary magnetic field is directed at an angle to the solar wind velocity.

Keywords: solar wind, interplanetary magnetic field, planetary bow shock, Mach cone.

INTRODUCTION

Since detailed magnetohydrodynamic (MHD) or kinetic calculations of the position and shape of planetary bow shocks (BS) are cumbersome, consume too much time, and therefore cannot be used to track BS motion in real time, empirical models are usually used in studies [Fairfield, 1971; Formisano, 1979; Slavin, Holzer, 1981; Němeček, Šafránková, 1991; Peredo et al., 1995; Fairfield et al., 2001; Chapman, Cairns, 2003; Jelínek et al., 2012; Meziane et al., 2014]. Nonetheless, such models can be applied in the area of solar wind parameters used for their construction, and are limited in space by the region in which measurements are made. M.I. Verigin has developed a method of physical analytical modeling, which relies on theoretical expressions with a small number of free parameters [Verigin et al., 1999; Verigin et al., 1997, 2001a, b, 2003a, b; Verigin, 2004; Kotova et al., 2005]. The parameters are determined from comparison with experimental data or with numerical solutions. The analytical models can easily be used to describe a variety of phenomena in planetary space under any solar wind conditions.

An analytical model of BS for obstacles of different shapes in the gas-dynamic (GD) approximation is presented [Verigin et al., 2003a]. This model with an exact analytical solution for a BS inclination angle at an infinite distance to direction of the undisturbed solar wind [Verigin et al., 2003b] is utilized to build a BS model in the MHD approximation.

COORDINATE SYSTEM AND SKEWING ANGLE OF A BOW SHOCK

Bow shocks are described using the Geocentric InterPlanetary Medium (GIPM) coordinate system. In this coordinate system, the X-axis is opposite to the direction of the undisturbed solar wind. The Y-axis is directed so that the interplanetary magnetic field (IMF) vector lies in the second — fourth quadrants of the XY plane. The Z-axis completes the coordinate system to the right [Bieber, Stone, 1979]. To simulate a shock wave forming in a supersonic super-Alfvenic upcoming plasma flow near obstacles of different shapes, we have used detailed MHD calculations made at the University of Michigan. The calculations were performed for obstacles of two types: a hemisphere with an elongated tail and a cylindrical paraboloid of revolution. All the calculations were carried out in units of the distance to the magnetopause r_o.

In the GD approximation when a gas (plasma) flows around an axisymmetric obstacle, which is directed along its axis, the BS shape is axisymmetric. The presence of IMF in the solar wind flow leads to an additional (compared to the aberration due to the orbital motion of

This is an open access article under the CC BY-NC-ND license

the planet) skewing of the BS nose point from the X-axis in the XY plane of the GIPM coordinate system. If we define the nose of the MHD BS as the point at which the plasma behind BS flows along the normal to the front, the Rankine-Hugoniot conditions allow us to obtain a relation for the angle of plasma skewing at the nose point α_{vn} [Verigin, 2004]. We will call this angle between the direction of the upcoming flow and the normal to the BS surface at the nose point a skewing angle of BS:

$$\mathrm{tg}\ \alpha_{vn} = \frac{(1-\varepsilon)\sin 2(\vartheta_{bv}-\alpha_{vn})}{2\left(\varepsilon M_A^2\cos^2\alpha_{vn}-\cos^2\left(\vartheta_{bv}-\alpha_{vn}\right)\right)}, \qquad (1)$$

where ε is the value inverse to the gas density jump at the BS front. In the case of the magnetogasdynamics, $\varepsilon=\varepsilon(\gamma, M_A, M_S, \alpha_{vn}, \vartheta_{bn})$, where α_{vn} and ϑ_{bn} are the angles between the normal to BS and the plasma flow direction or the magnetic field respectively. A cubic equation to determine ε has been derived in [Petrinec, Russell, 1997, Equation (12)]. The skewing angle depends on the angle ϑ_{bv} between IMF and SW directions, Alfvén M_A and sonic M_S Mach numbers. The effect disappears for flows with magnetic fields parallel or perpendicular to the plasma flow. For typical conditions in the near-Earth solar wind, the skewing angle is ~5° and may reach 20°–30° at small M_A.

METHOD OF FITTING THE PLANETARY BS BY AN ANALYTICAL EXPRESSION

When constructing an analytical model of planetary BS for cases where IMF is parallel or perpendicular to the plasma upstream, Kotova et al. [2020] have used the following expression to describe its shape and position:

$$\rho^2(x) = 2R_s(r_s-x) + \mathrm{tg}^2\omega_{as}(r_s-x)^2\left(1+\frac{\frac{b_s}{\mathrm{tg}^2\omega_{as}}-1}{1+d_s\frac{r_s-x}{R_s}}\right), \qquad (2)$$

where $\rho=(y^2+z^2)^{1/2}$; r_s is the distance to BS at a subsolar (nose) point; R_s is the radius of curvature; b_s is the BS bluntness at the nose point; ω_{as} is the asymptotic inclination of BS defining the asymptotic Mach number $M_{as}=1/\sin^2\omega_{as}$. Bluntness is a dimensionless parameter characterizing the BS shape. The nose part of BS is close in shape to an blunt ellipsoid at $b_s<-1$ and to a elongated ellipsoid at $-1<b_s<0$; it is spherical at $b_s=-1$, parabolic at $b_s=0$, and hyperbolic at $b_s>0$. The parameter d_s characterizes the transition from the dominance of parameters of the BS subsolar region to the dominance of parameters of the region where the main role belongs to the asymptotic slope of the shock. For an arbitrary direction of IMF, the BS shape has a unique symmetry with respect to the XY plane containing vectors of IMF and upcoming flow velocity; and parameters of Expression (2), except for r_s, depend on the clock angle φ. In this general case, BS should be considered in a coordinate system such that X_s and Y_s are turned by α_{vn} relative to X_{GIPM} and Y_{GIPM} clockwise. In this coordinate system turned by the skewing angle, we can also obtain an exact analytical solution of MHD equations for ω_{as} at an arbitrary angle ϑ_{bv} [Verigin et al., 2003b], and we can still use Expression (2) for fitting BS.

In the case when the magnetic field vector is perpendicular to the flow velocity vector, for the radius of curvature and bluntness the following expressions have been used [Kotova et al., 2020]:

$$R_s(\varphi) = \frac{R_{sy}R_{sz}}{R_{sy}\sin^2\varphi + R_{sz}\cos^2\varphi}, \qquad (3)$$
$$b_s(\varphi) = b_{sz}\sin^2\varphi + b_{sy}\cos^2\varphi,$$

where R_{sy}, R_{sz} are the radii of curvature, and b_{sy}, b_{sz} are the bluntnesses at the subsolar point of the shock surface in the planes XY, i.e. when $\varphi=0°$, and XZ, i.e. when $\varphi=90°$, respectively. We will use these expressions for an arbitrary direction of IMF too. For now, let us regard d_s as independent of φ.

So, fitting the BS surface by Expression (2) requires us to determine seven parameters: α_{vn}, r_s, R_{sy}, R_{sz}, b_{sy}, b_{sz}, d_s.

Figure 1 presents an example of the fitting of BS calculated in the MHD approximation near a spherically cylindrical obstacle. Parameters of the fitting are $\alpha_{vn}=4.0°$, $r_s=1.33$, $R_{sy}=1.79$, $R_{sz}=1.82$, $b_{sy}=-0.33$, $b_{sz}=-0.14$, $d_s=1.05$. Obviously, there is good agreement between the analytical fitting and MHD calculations.

DETERMINING PARAMETERS OF THE ANALYTICAL MHD APPROXIMATION OF BS FROM GD CALCULATIONS

To find general expressions for the fitting parameters, we will use a gas-dynamic analytical model of BS, which quite accurately describes its position near obstacles of different shapes [Verigin et al., 2003a]. Formulas for calculating GD parameters are given in Appendix 1. Kotova et al. [2020] have derived formulas for recalculation of GD parameters in MHD for flows with magnetic fields parallel or perpendicular to the plasma flow. These formulas include an additional factor Γ arising when considering the expansion of the central flow tube behind BS for the MHD flow as compared to the GD flow. For the GD flow, the relative expansion rate of the central flow tube is described by the following equation:

$$\frac{1}{S}\frac{dS}{dx} = -\frac{2}{R_s}\frac{1-\varepsilon}{\varepsilon} = \frac{1}{\rho V}\frac{d(\rho V)}{dx}.$$

For the MHD flow, this expression can be written as follows:

$$\frac{1}{S}\frac{dS}{dx} = -\frac{R_{sy}+R_{sz}}{R_{sy}R_{sz}}\frac{1-\varepsilon}{\varepsilon}\frac{1}{\Gamma},$$

where $\Gamma=\Gamma(\varepsilon, \gamma, M_A, M_S, \vartheta_{bv}, \alpha_{vn})$; γ is the polytropic index (see Appendix 2). When calculating the MHD parameters r_s, R_s, b_s, we use the same formulas from [Verigin et al., 2003a] as a basis, but with the compression ratio ε calculated in the MHD approximation and

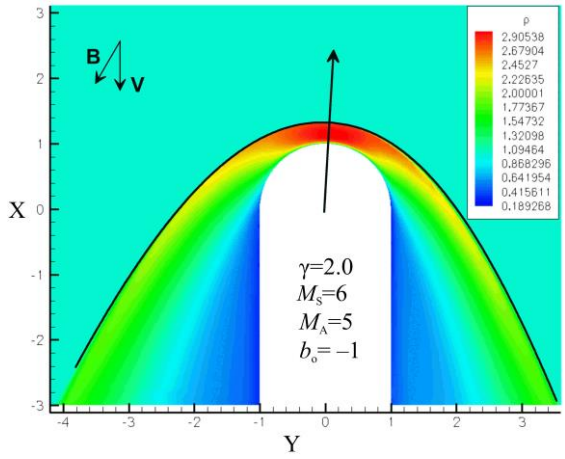

Figure 1. Position and shape of BS (in the $X_{GIPM}Y_{GIPM}$ plane) generated in the upstream solar wind with a magnetic field directed at an angle of 30° to the flow velocity. The thick line indicates fitting by (2). The long arrow shows the direction of the normal to BS at the nose point

with $\varepsilon^*=\varepsilon/(\varepsilon-1)$ replaced by $\varepsilon^*\Gamma$, and with M_S replaced by $M_{as}=(1+1/\mathrm{tg}^2\,\omega)^{1/2}$.

Figure 2, *a* demonstrates that at any direction of the magnetic field the distance to the BS nose point $r_{s\ norm}$ can be found from the formula obtained in [Kotova et al., 2020]:

$$r_{s\ norm}-r_o=\Gamma^{2/3}\times$$
$$\times(r_{s_{GD}}((\Gamma\varepsilon/(1-\varepsilon)),\gamma,R_o,b_o)-r_o)\chi(\vartheta_{bv}),$$
$$\chi(\vartheta_{bv})=1+0.37\sin\vartheta_{bv},$$

where R_o is the radius of curvature; b_o is the bluntness of an obstacle at a subsolar point, $r_{s_{GD}}$ is the distance to the BS nose point calculated in the GD approximation with ε^* replaced by $\Gamma\varepsilon^*$ [Verigin et al., 2003a]. Similarly, the formulas for the radii of curvature of the BS surface near the nose point coincide with those obtained previously for particular cases of IMF directions:

$$R_{sy\ norm}=\Gamma^{-2/3}R_{s_{GD}}(\varepsilon\Gamma,\gamma,R_o,b_o)(M_{asy}/M_{asz})^{1/2},$$
$$R_{sz}=R_{sy}\Gamma^{\sin\vartheta_{bv}/2},$$

where asymptotic Mach numbers in the directions *y* and *z*:

$$M_{asy}^2=\frac{1}{\mathrm{tg}^2(\omega_y)}+1,$$
$$M_{asz}^2=\frac{1}{\mathrm{tg}^2(\omega_z)}+1.$$

For conversion of the GD parameters b_s and d_s to the respective MHD parameters, only preliminary relations have been obtained.

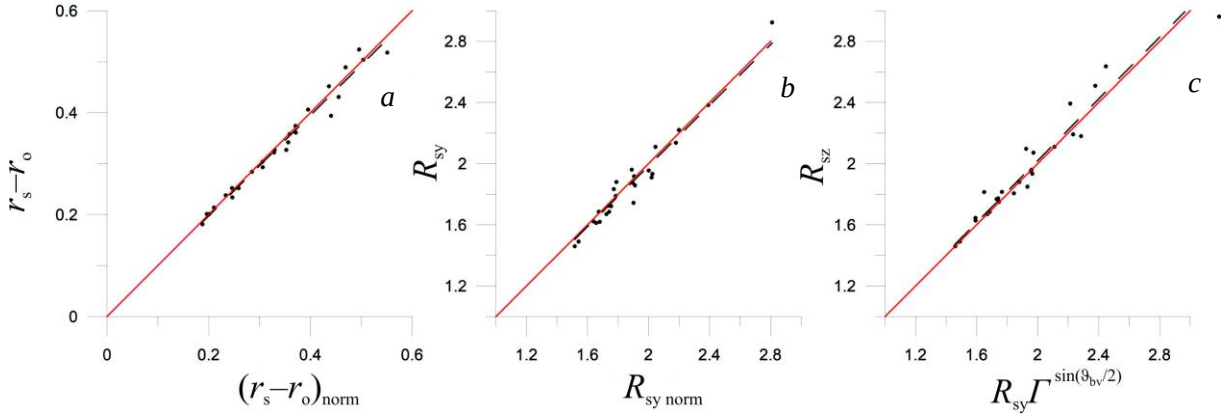

Figure 2. Comparison of parameters of bow shock model (2) fitting MHD calculations with parameters of the GD model (Appendix 1)

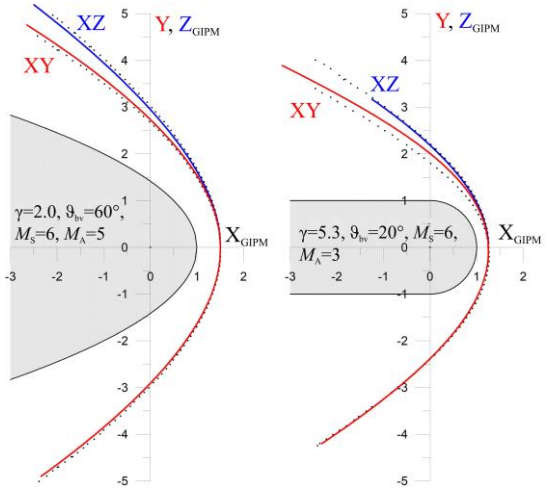

Figure 3. Position and shape of BS formed near two different obstacles in the XY and XZ planes: dots mark an MHD calculation; solid lines indicate fitting (2) with parameters recalculated using GD formulas

Figure 3 presents two examples of the position and shape of the bow shock, defined using the renormalized GD formulas (b_s and d_s were recalculated by the formulas for the magnetic field perpendicular to the direction of the plasma stream [Kotova et al., 2020]).

CONCLUSIONS

The presence of the interplanetary magnetic field in the solar wind flow leads to an additional inclination of the BS nose point from the aberrated X-axis in the $X_{GIPM}Y_{GIPM}$ plane of the GIPM coordinate system. We have shown that for any direction of the magnetic field vector relative to the plasma flow velocity vector the surface of the planetary bow shock can be fitted by an analytical function with four–seven free parameters that have a clear physical meaning: the distance to the nose point, the radii of curvature and bluntnesses at the nose point in the XY and XZ planes, the parameter of transition to the asymptotic downstream slope, and the skewing angle. The parameters can be converted from the gas-dynamic approximation.

REFERENCES

Bieber J.W., Stone E.C. Energetic electron bursts in the magnetopause electron layer and in interplanetary space / Magnetospheric Boundary Layers — A Sydney Chapman Conference / ESA SP-148. 1979, p. 131.

Chapman J.F., Cairns I.H. Three-dimensional modeling of Earth's bow shock: Shock shape as a function of Alfvén Mach number. *J. Geophys. Res*. 2003. V. 108, iss. A05, 1174. DOI: 10.1029/2002JA009569.

Fairfield D.H. Average and unusual locations of the Earth's magnetopause and bow shock. *J. Geophys. Res*. 1971, vol. 76, no. 28, pp. 6700–6716.

Fairfield D.H., Cairns I.H., Desch M.D., Szabo A., Lazarus A.J., Aellig M.R. The location of low Mach number bow shocks at Earth. *J. Geophys. Res*. 2001, vol. 106, no. A11, pp. 25361–25376.DOI: 10.1029/2000JA000252.

Formisano V. Orientation and shape of the Earth's bow shock in three dimensions. *Planet. Space Sci*. 1979, vol. 27, p. 1151.

Jelínek K., Němeček Z., Šafránková J. A new approach to magnetopause and bow shock modeling based on automated region identification. *J. Geophys. Res*. 2012. V. 117, A05208. DOI: 10.1029/2011JA017252.

Kotova G., Verigin M., Zastenker G., Nikolaeva N., Smolkin B., Slavin J., Szabo A., Merka J., Nemechek Z., Safrankova J. Bow shock observations by Prognoz–Prognoz 11 data: analysis and model comparison. *Adv. Space Res*. 2005, vol. 36, pp. 1958–1963. DOI: 10.1016/j.asr.2004.09.007.

Kotova G., Verigin M., Gombosi T., Kabin K., Bezrukikh V.V. Analytical description of the near planetary bow shock based on gas-dynamic and magneto-gas–dynamic modeling for the magnetic field parallel and perpendicular to the plasma flow. *Geomagnetism and Aeronomy*. 2020, vol. 60, pp. 162–170. DOI: 10.1134/S0016793220020073.

Meziane K., Alrefay T.Y., Hamza A. On the shape and motion of the earth's bow shock. *Planet. Space Sci*. 2014, vol. 93-94, pp. 1–9. DOI: 10.1016/j.pss.2014.01.006.

Němeček Z., Šafránková J. The Earth's bow shock and magnetopause position as a result of solar wind-magnetosphere interaction. *J. Atmos. Terr. Phys*. 1991, vol. 53, iss. 11-12, pp. 1049–1054. DOI: 10.1016/0021-9169(91)90051-8.

Peredo M., Slavin J.A., Mazur E., Curtis S.A. Three-dimensional position and shape of the bow shock and their variation with Alfvénic, sonic and magnetosonic Mach numbers and interplanetary magnetic field orientation. *J. Geophys. Res*. 1995, vol. 100, no. A5, pp. 7907–7916. DOI: 10.1029/94JA02545.

Petrinec S.M., Russell C.T. Hydrodynamic and MHD equations across the bow shock and along the surfaces of planetary obstacles. *Space Sci. Rev*. 1997, vol. 79, pp. 757–791. DOI: 10.1023/A:1004938724300.

Slavin J.A., Holzer R.E. Solar wind flow about the terrestrial planets. 1. Modeling bow shock position and shape. *J. Geophys. Res*. 1981, vol. 86, no. A13, pp. 11401–11418.

Verigin M.I. Location and shape of near-planetary bow shocks: gas-dynamical and MHD aspects. *Solnechno-zemnye svyazi i elektromagnitnye predvestniki zemletryasenii: sbornik dokladov III Mezhunarodnoi konferentsii* [*Solar-Terrestrial and Electromagnetic Precursors of Earthquakes*. *Proceedings of the International Conference, 16–21 August 2004, Petropavlovsk-Kamchatskii*]. 2004, pp. 49–69. (In Russian).

Verigin M.I., Kotova G.A., Remizov A.P., Shutte N.M., Schwingenschuh K., Riedler W., Zhang T.L., Rosenbauer H., Szegö K., Tatrallyay M., Styazhkin V. Studies of the Martian bow shock response to the variation of the magnetosphere dimensions according to TAUS and MAGMA measurements aboard the Phobos 2 orbiter. *Adv. Space Res*. 1997, vol. 20, no. 2, pp. 155–158. DOI: 10.1016/S0273-1177(97)00526-7.

Verigin M.I., Kotova G.A., Remizov A.P., et al. Shape and location of planetary bow shocks. *Cosmic Res*. 1999, vol. 37, no. 1, pp. 34–39.

Verigin M., Kotova G., Szabo A., Slavin J., Gombosi T., Kabin K., Shugaev F., Kalinchenko A. Wind observations of the terrestrial bow shock 3-D shape and motion. *Earth, Planets and Space*. 2001a, vol. 53, no. 10, pp. 1001–1009. DOI: 10.1186/BF03351697.

Verigin M.I., Kotova G.A., Slavin J., Szabo A., Kessel M., Safrankova J., Nemecek Z., Gombosi T.I., Kabin K., Shugaed F., Kalinchenko A. Analysis of the 3-D shape of the terrestrial bow shock by Interball/Magion 4 observations. *Adv. Space Res*. 2001b, vol. 28, no. 6, pp. 857–862. DOI: 10.1016/S0273-1177(01)00502-6.

Verigin M., Slavin J., Szabo A., Gombosi T., Kotova G., Plochova O., Szegö K., Tátrallyay M., Kabin K., Shugaev F. Planetary bow shocks: Gasdynamic analytic approach. *J. Geophys. Res*. 2003a. V. 108, iss. A08, 1323. DOI: 10.1029/2002JA009711.

Verigin M., Slavin J., Szabo A., Kotova G., Gombosi T. Planetary bow shocks: Asymptotic MHD Mach cones. *Earth, Planets and Space*. 2003b, vol. 55, pp. 33–38. DOI: 10.1186/BF03352460.

How to cite this article

Kotova G.A., Verigin M.I., Gombosi T., Kabin K. Analytical model of the planetary bow shock for various magnetic field directions based on MHD calculations. *Solar-Terrestrial Physics*. 2020. Vol. 6. Iss. 4. P. 44–49. DOI: 10.12737/stp-64202007.

APPENDIX 1

Formulas for calculating the position and shape of the planetary bow shock in the GD approximation

Equations (34)– (38) and (39)–(43) are from [Verigin et al., 2003a] (in (36) there is a misprint, corrected in the review by Verigin (2004), before the second term there should be "+" instead of "–").

$$\varepsilon^* = \frac{\varepsilon}{1-\varepsilon},$$

$$\xi = \varepsilon^* + \frac{\gamma+1}{50}\left(\varepsilon^* - \frac{\gamma-1}{2}\right),$$

$$r_s = r_o + \frac{1.229c(b_o)R_o\xi^{2/3}}{\left(1+\frac{\gamma+1}{50}\right)^{2/3}(\gamma+1)^{1/3}}\left(1-\frac{b(b_o,\gamma)}{\xi^{1/6}}\right),$$

$$R_s = 3c(b_o)R_o\xi^{5/3}\left(\frac{1}{(1+\gamma)^{4/3}\left(1+\frac{\gamma+1}{50}\right)^{5/3}} + \frac{a(b_o,\gamma)}{\xi^{d(b_o)}}\right),$$

$$b_s = \frac{1}{M_S^2-1} + e(b_o,\gamma) + \frac{M_S^2+1}{M_S^4}\ \frac{\frac{21}{17}\left(e(b_o,\gamma)\right)^2 - \frac{14}{9}e(b_o,\gamma) + \frac{7}{4}}{1-\frac{23}{30}e(b_o,\gamma)},$$

$$d_s = \exp\left(\frac{107}{29} - \frac{371}{68}\left(\frac{8}{13}\left(b_o - \frac{4}{21}\right) + \left(1+\left|\frac{8}{13}\left(b_o-\frac{4}{21}\right)\right|^{11/7}\right)^{7/11}\right)\right),$$

where

$$a(b_o,\gamma) = \frac{1}{2}\left(\frac{52}{25} + \frac{97}{84} - \frac{33}{10}\left(\frac{1}{(\gamma+1)^{\frac{13}{4}}} - \left(\frac{5}{12}\right)^{\frac{13}{4}}\right)\right)\left(1-\frac{\frac{7}{16}b_o}{\left(1+\left|\frac{7}{16}b_o\right|^{\frac{8}{33}}\right)^{\frac{33}{8}}}\right) - \frac{97}{84} + \frac{33}{10}\left(\frac{1}{(\gamma+1)^{\frac{13}{4}}} - \left(\frac{5}{12}\right)^{\frac{13}{4}}\right),$$

$$b(b_o,\gamma) = \frac{1}{2}\left(-\frac{23}{35} + \frac{43}{3}\left(\frac{1}{(\gamma+1)^{\frac{68}{13}}} - \left(\frac{5}{12}\right)^{\frac{68}{13}}\right) - \frac{24}{13} + \frac{13}{18}\left(\frac{1}{\gamma^{\frac{57}{13}}} - \left(\frac{5}{7}\right)^{\frac{57}{13}}\right)\right)\times$$

$$\times\left(1-\frac{b_o-\frac{3}{10}}{\left(\left(\frac{119}{20}\right)^{\frac{1}{2}} + \left|b_o-\frac{3}{10}\right|^{\frac{1}{2}}\right)^2}\right) + \frac{24}{13} - \frac{13}{18}\left(\frac{1}{\gamma^{\frac{57}{13}}} - \left(\frac{5}{7}\right)^{\frac{57}{13}}\right),$$

$$c(b_o) = \frac{6}{5}\left(\frac{17}{20}b_o + \left(1+\left|\frac{17}{20}b_o\right|^{\frac{5}{3}}\right)^{\frac{3}{5}}\right) + \frac{\frac{41}{52}}{\left(\left(\frac{26}{9}\right)^2 + b_o^{\,2}\right)^{\frac{1}{4}}},$$

$$d(b_o) = \frac{1}{2}\left(\frac{85}{47} - \frac{15}{29}\right)\left(1-\frac{19}{33}\frac{\left(b_o-\frac{39}{70}\right)}{\left(1+\left|\frac{19}{33}\left(b_o-\frac{39}{70}\right)\right|^{\frac{5}{6}}\right)^{\frac{6}{5}}}\right) + \frac{15}{29},$$

$$e\left(b_{\rm o},\gamma\right)=\frac{1}{2}\left(-\frac{1042}{17}-40\left(\frac{1}{\gamma^{\frac{15}{4}}}-\left(\frac{5}{7}\right)^{\frac{15}{4}}\right)-\frac{1318}{39}\right)\left(1-\frac{\left(b_{\rm o}+\frac{841}{61}+\frac{160}{11}\left(\frac{1}{\gamma^{\frac{16}{5}}}-\left(\frac{5}{7}\right)^{\frac{16}{5}}\right)\right)}{\left(\left(\frac{809}{18}\right)^2+\left(b_{\rm o}+\frac{841}{61}+\frac{160}{11}\left(\frac{1}{\gamma^{\frac{16}{5}}}-\left(\frac{5}{7}\right)^{\frac{16}{5}}\right)\right)^2\right)}\right)+\frac{1318}{39}.$$

APPENDIX 2

Equations for the parameter Γ in the MHD approximation

$$\frac{1}{\Gamma}=\frac{\varepsilon M_{\rm A}^2\cos^2\alpha_{\rm vn}}{\varepsilon M_{\rm A}^2\cos^2\alpha_{\rm vn}-\cos^2\left(\vartheta_{\rm bv}-\alpha_{\rm vn}\right)}-$$

$$-\frac{\sin\left(\vartheta_{\rm bv}-\alpha_{\rm vn}\right)\left(\sin\left(\vartheta_{\rm bv}-\alpha_{\rm vn}\right)+{\rm tg}\,\alpha_{\rm vn}\cos\left(\vartheta_{\rm bv}-\alpha_{\rm vn}\right)\right)\left(\varepsilon M_{\rm A}^2\cos^2\alpha_{\rm vn}+\cos^2\left(\vartheta_{\rm bv}-\alpha_{\rm vn}\right)\right)}{\left(\varepsilon M_{\rm A}^2\cos^2\alpha_{\rm vn}-\cos^2\left(\vartheta_{\rm bv}-\alpha_{\rm vn}\right)\right)^2}-$$

$$-\frac{1}{1-\varepsilon}\quad\frac{\cos\left(\vartheta_{\rm bv}-\alpha_{\rm vn}\right)\sin\left(\vartheta_{\rm bv}-\alpha_{\rm vn}\right)\left(M_{\rm A}^2\cos^2\alpha_{\rm vn}-\cos^2\left(\vartheta_{\rm bv}-\alpha_{\rm vn}\right)\right)}{\left(\varepsilon M_{\rm A}^2\cos^2\alpha_{\rm vn}-\cos^2\left(\vartheta_{\rm bv}-\alpha_{\rm vn}\right)\right)^2}\zeta,$$

where $\zeta=\dfrac{a_1\varepsilon^3+b_1\varepsilon^2+c_1\varepsilon+d_1}{3a\varepsilon^2+2b\varepsilon+c}$ with parameters

$$a=\left(\gamma+1\right)M_{\rm A}^6\cos^6\alpha_{\rm vn},$$

$$b=-\left(\gamma-1\right)M_{\rm A}^6\cos^6\alpha_{\rm vn}-\left(\gamma+2\right)M_{\rm A}^4\cos^4\alpha_{\rm vn}\cos^2\left(\vartheta_{\rm bv}-\alpha_{\rm vn}\right)-\left(\gamma+2\left(\frac{M_{\rm A}}{M_{\rm S}}\right)^2\right)M_{\rm A}^4\cos^4\alpha_{\rm vn},$$

$$c=\left(\gamma-2+\gamma\cos^2\left(\vartheta_{\rm bv}-\alpha_{\rm vn}\right)\right)M_{\rm A}^4\cos^4\alpha_{\rm vn}+\left(\gamma+1+4\left(\frac{M_{\rm A}}{M_{\rm S}}\right)^2\right)M_{\rm A}^2\cos^2\alpha_{\rm vn}\cos^2\left(\vartheta_{\rm bv}-\alpha_{\rm vn}\right),$$

$$a_1=-6\left(\gamma+1\right)M_{\rm A}^6\cos^5\alpha_{\rm vn}\sin\alpha_{\rm vn},$$

$$b_1=2M_{\rm A}^4\cos^3\alpha_{\rm vn}\left(\left(3\left(\gamma-1\right)M_{\rm A}^2\cos^2\alpha_{\rm vn}+2\left(\gamma+2\right)\cos^2\left(\vartheta_{\rm bv}-\alpha_{\rm vn}\right)+2\gamma+4\left(\frac{M_{\rm A}}{M_{\rm S}}\right)^2\right)\times\right.$$

$$\left.\times\sin\alpha_{\rm vn}-\left(\gamma+2\right)\cos\alpha_{\rm vn}\cos\left(\vartheta_{\rm bv}-\alpha_{\rm vn}\right)\sin\left(\vartheta_{\rm bv}-\alpha_{\rm vn}\right)\right),$$

$$c_1=-2M_{\rm A}^2\cos\alpha_{\rm vn}\left(\left(2\left(\gamma-2\right)M_{\rm A}^2\cos^2\alpha_{\rm vn}+2\gamma M_{\rm A}^2\cos^2\alpha_{\rm vn}\cos^2\left(\vartheta_{\rm bv}-\alpha_{\rm vn}\right)+\left(1+\gamma+4\left(\frac{M_{\rm A}}{M_{\rm S}}\right)^2\right)\cos^2\left(\vartheta_{\rm bv}-\alpha_{\rm vn}\right)\right)\times\right.$$

$$\left.\times\sin\alpha_{\rm vn}-\left(\gamma M_{\rm A}^2\cos^2\alpha_{\rm vn}+1+\gamma+4\left(\frac{M_{\rm A}}{M_{\rm S}}\right)^2\right)\cos\alpha_{\rm vn}\cos\left(\vartheta_{\rm bv}-\alpha_{\rm vn}\right)\sin\left(\vartheta_{\rm bv}-\alpha_{\rm vn}\right)\right),$$

$$d_1=2\cos\left(\vartheta_{\rm bv}-\alpha_{\rm vn}\right)\times$$

$$\times\left(\left(\gamma-1\right)\cos\alpha_{\rm vn}\cos\left(\vartheta_{\rm bv}-\alpha_{\rm vn}\right)\sin\alpha_{\rm vn}-\left(\left(\gamma-1\right)M_{\rm A}^2\cos^2\alpha_{\rm vn}+4\left(\frac{M_{\rm A}}{M_{\rm S}}\right)^2\cos^2\left(\vartheta_{\rm bv}-\alpha_{\rm vn}\right)\right)\sin\left(\vartheta_{\rm bv}-\alpha_{\rm vn}\right)\right).$$